Quantum chaos of unitary Fermi gases in the strong pairing fluctuation region

Xinloong Han[1] and Boyang Liu[2,*]

[1]*Department of Physics and Center of Theoretical and Computational Physics, The University of Hong Kong, Hong Kong, China*

[2]*Institute of Theoretical Physics, Beijing University of Technology Beijing 100124, China*

(Received 9 March 2020; revised 27 May 2020; accepted 22 June 2020; published 17 July 2020)

The growth rate of the out-of-time-ordered correlator in a N-flavor Fermi gas is investigated and the Lyapunov exponent λ_L is calculated to the order of $1/N$. We find that the Lyapunov exponent monotonically increases as the interaction strength increases from the BCS limit to the unitary region. At the unitarity, the Lyapunov exponent increases while the temperature drops and it can reach to the order of $\lambda_L \sim T$ around the critical temperature for the $N = 1$ case. For $N \to \infty$, the Lyapunov exponent reaches its maximum $\lambda_L \approx 4.35T/N$ at the critical temperature. The system scrambles faster for stronger pairing fluctuations. At the BCS limit, the Lyapunov exponent behaviors as $\lambda_L \propto e^{\mu/T} a_s^2 T^2/N$.

DOI: 10.1103/PhysRevB.102.045123

I. INTRODUCTION

Information scrambling is a crucial stage in thermalization of a closed system. During this process, the quantum entanglement spreads across all the freedoms of the system and the memory of the initial state is lost, which is taken as a key prerequisite for thermalization. Recently, studies in gauge-gravity duality have inspired insights into quantum chaos [1–8]. It is suggested that black holes are the fastest scramblers in nature [1]. Moreover, the experimental realizations of nearly isolated quantum systems also attract increasing attention to this area [9–11]. Analogous to the Lyapunov exponents describing the growth of chaos in classical models, the scrambling to the quantum chaos can also be probed by the growth rate of the so-called out-of-time-ordered correlator (OTOC).

The OTOC was first introduced by Larkin and Ovchinnikov in the study of superconductivity [12]. Recently, this subject was revived by the discovery of an unexpected bound on the Lyapunov exponent that is extracted from OTOCs [1,13]. Several experiments on measurements of OTOCs have been conducted [14–17]. Usually, instead of directly calculating the OTOC, it's more convenient to evaluate the "regulated" squared commutator defined as $\mathcal{C}(t) = \mathrm{Tr}\{\sqrt{\rho}[W(t), V(0)]^\dagger \sqrt{\rho}[W(t), V(0)]\}$ [18,19], where $\rho = e^{-\beta H}$ is the thermal density matrix and W and V are local Hermitian operators in general. It can be expanded as $\mathcal{C}(t) = 2\mathrm{Tr}\{\sqrt{\rho}W(t)V(0)\sqrt{\rho}V(0)W(t)\} - 2\mathrm{Re}[\mathrm{Tr}\{\sqrt{\rho}W(t)V(0)\sqrt{\rho}W(t)V(0)\}]$. The first term is time ordered. On the other hand, the second term is on an unusual time order as illustrated in Fig. 1 and it's called an OTOC. In a chaotic system, $\mathcal{C}(t)$ is expected to have an exponential behavior at the timescale t_L as $\mathcal{C}(t) \sim e^{\lambda_L t}$. Analogous to the classical chaos, λ_L is called the Lyapunov exponent and $t_L^{-1} \sim \lambda_L$. Based on some reasonable physical assumption, the Lyapunov exponent is proven to have an upper bound of $2\pi k_B T/\hbar$ and it saturates in models with gravity duals [1,13]. An concrete example is the celebrated Sachdev-Ye-Kitaev model [20–22] which holds a conformal symmetry in the low-energy limit and is dual to an AdS_2 gravity theory.

In condensed-matter physics, the systems usually don't possess conformal symmetry. However, there exist some exceptions. At the critical point, the conformal symmetry can emerge for low energy and long distance. Investigations have been done in this regime [19,23,24]. In these system, there are no quasiparticle excitations and the temperature is the only relevant scale. The Lyapunov exponents are found to obey the relationship of $\lambda_L \sim \kappa T$. The unitary Fermi gas is another example with scaling invariance. With the properties of being highly controllable and hyperclean, it can be a perfect playground to investigate information scrambling [25,26] and thermalization in closed quantum systems. At the unitary point, the nonrelativistic conformal symmetry emerges and investigations have been taken to discuss its duality to a gravity theory [27,28]. The behaviors of the Lyapunov exponent in unitary Fermi gases have been studied in Ref. [29]. They used the method of high-temperature expansion to investigate the region of $z \ll 1$, where $z = e^{\beta\mu}$ is the fugacity. They also used the effective field theory to study the region of low temperature deep in the superfluid phase. However, the region close to the critical temperature has not been investigated, where the fugacity $z > 1$. This region is more interesting since it has been shown that around this region the system may demonstrate some non-Fermi liquid behaviors [30–33].

In this paper, we calculate the Lyapunov exponent of a N-flavor Fermi gas with tunable interaction in the region close to the critical temperature. The OTOC is evaluated by a series of ladder diagrams and the Lyapunov exponent is calculated to the order of $1/N$. As the interaction strength increases from the BCS limit to the unitary regime, we find that the Lyapunov exponent monotonically increases while the temperature is fixed. We also investigate the temperature dependence of the Lyapunov exponent at the unitarity. λ_L can increase to $\lambda_L \sim T$ for $N = 1$ case when the temperature is close to the critical temperature. For $N \to \infty$, the Lyapunov

*boyangleo@gmail.com

exponent reaches its maximum $\lambda_L \approx 4.35T/N$ at the critical temperature. Furthermore, we also find that the Lyapunov exponent behaves as $\lambda_L \propto z a_s^2 T^2/N$ for high temperature at the BCS limit, where $a_s \to 0^-$.

II. MODEL

We will start from a system with N fermion flavors. The Hamiltonian can be cast as

$$\hat{H} = \int d^3\mathbf{r}\Big\{\sum_{i\sigma}\hat{\psi}^\dagger_{i\sigma}(\mathbf{r})\Big(-\frac{\nabla^2}{2m}-\mu\Big)\hat{\psi}_{i\sigma}(\mathbf{r}) - \frac{g}{N}\sum_{ij}\hat{\psi}^\dagger_{i\uparrow}(\mathbf{r})\hat{\psi}^\dagger_{i\downarrow}(\mathbf{r})\hat{\psi}_{j\downarrow}(\mathbf{r})\hat{\psi}_{j\uparrow}(\mathbf{r})\Big\}, \tag{1}$$

where $\psi_{i\sigma}(\psi^\dagger_{i\sigma})$ is the annihilation (creation) operator of the fermion field with flavor i and spin σ. Parameter g is the bare interaction strength between the fermions. Here we assume the interaction strengths between different flavors are the same and can be related to an s-wave scattering length a_s by the following renormalization relation:

$$\frac{1}{g} = -\frac{m}{4\pi a_s} + \int \frac{d^3\mathbf{k}}{(2\pi)^3}\frac{1}{2\epsilon_\mathbf{k}}, \tag{2}$$

where $\epsilon_\mathbf{k} = k^2/2m$ and m is the mass of the fermions. By introducing an auxiliary bosonic field φ, the four-fermion interaction term can be decoupled through the Hubbard-Stratonovich transformation. Then, in the imaginary time path integral formulism, the partition function can be written as $\mathcal{Z} = \int \mathcal{D}[\psi_{i\sigma}, \psi^\dagger_{i\sigma}, \varphi, \bar{\varphi}]e^{-S[\psi_{i\sigma},\psi^\dagger_{i\sigma},\varphi,\bar{\varphi}]}$, where the action S is

$$S[\psi_{i\sigma}, \psi^\dagger_{i\sigma}, \varphi, \bar{\varphi}] = \int d\tau d^3\mathbf{r}\Big(\sum_{i\sigma}\psi^\dagger_{i\sigma}(\tau,\mathbf{r})\Big(\partial_\tau - \frac{\nabla^2}{2m}-\mu\Big)\psi_{i\sigma}(\tau,\mathbf{r}) - \sum_i \varphi\psi^\dagger_{i\uparrow}\psi^\dagger_{i\downarrow} - \sum_i \bar{\varphi}\psi_{i\downarrow}\psi_{i\uparrow} + \frac{N\bar{\varphi}\varphi}{g}\Big). \tag{3}$$

In this paper, we set $\hbar = 1$.

The imaginary time Greens' functions of fermions and bosons are defined as $\delta_{ij}\delta_{\sigma\sigma'}G(\tau,\mathbf{r}) = \langle\psi^\dagger_{i\sigma}(\tau,\mathbf{r})\psi_{j\sigma'}(0,0)\rangle$ and $\mathcal{G}(\tau,\mathbf{r}) = \langle\bar{\varphi}(\tau,\mathbf{r})\varphi(0,0)\rangle$, respectively. In the momentum space, the free propagators can be simply expressed as

$$G^{(0)}(i\omega^f_n,\mathbf{k}) = \frac{-1}{i\omega_n - \epsilon_\mathbf{k} + \mu}, \qquad \mathcal{G}^{(0)}(i\omega^b_n,\mathbf{k}) = g/N, \tag{4}$$

where $\omega^f_n = (2n+1)\pi/\beta$ and $\omega^b_n = 2n\pi/\beta$ are the Matsubara frequencies for fermions and bosons, respectively, and $\beta = 1/k_BT$. To calculate the Lyapunov exponent up to the order of $1/N$, we will involve the dressed propagators of fields ψ and φ as shown in Fig. 2. The dressed propagator of φ is a resummation of the bubble diagram. Then, it's written as

$$\mathcal{G}(i\omega^b_n,\mathbf{k}) = \frac{g/N}{1 - g\Pi(i\omega^b_n,\mathbf{k})}, \tag{5}$$

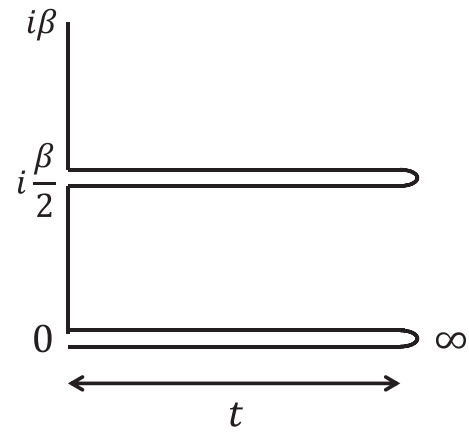

FIG. 1. The complex time contour for calculating the out-of-time-ordered correlators. The horizontal direction represents the real time evolution and the vertical direction represents the imaginary time evolution. It contains two real timefolds, which are separated by $i\beta/2$.

where $\Pi(i\omega^b_n,\mathbf{k})$ is the one-loop bubble:

$$\Pi(i\omega^b_n,\mathbf{q}) = \int \frac{d^3\mathbf{k}}{(2\pi)^3}\frac{1 - n_F(\epsilon_\mathbf{k}-\mu) - n_F(\epsilon_{\mathbf{q}-\mathbf{k}}-\mu)}{-i\omega^b_n + \epsilon_\mathbf{k} + \epsilon_{\mathbf{q}-\mathbf{k}} - 2\mu}. \tag{6}$$

$n_F(\epsilon_\mathbf{k}-\mu) = 1/\exp(\beta(\epsilon_\mathbf{k}-\mu)+1)$ is the Fermi-Dirac distribution function. The dressed propagator of field ψ_i is

$$G(i\omega^f_n,\mathbf{k}) = \frac{1}{-i\omega^f_n + \epsilon_\mathbf{k} - \mu - \Sigma(i\omega^f_n,\mathbf{k})}, \tag{7}$$

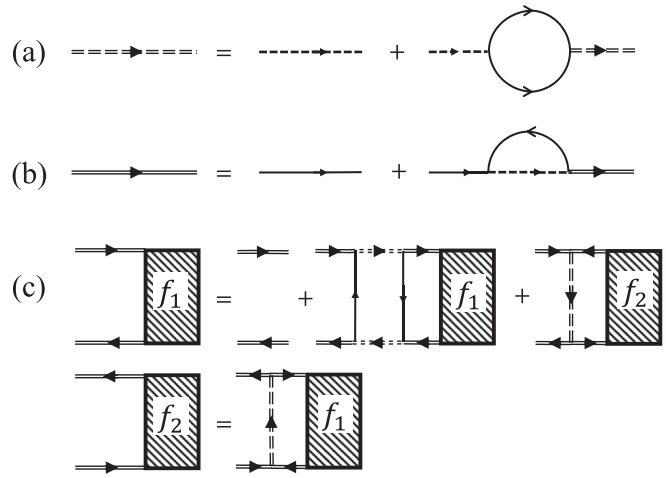

FIG. 2. (a) The Feynman diagram of the Dyson-Schwinger equation for field φ. (b) The Feynman diagram of the Dyson-Schwinger equation for field $\psi_{i\sigma}$. The double solid (dashed) line and the solid (dashed) line represent the dressed and free propagators of $\psi_{i\sigma}(\varphi)$, respectively. (c) The Feynman diagrams of the Bethe-Salpeter equations of the squared anticommutators.

where the self-energy of fermions $\Sigma(i\omega_n^f, \vec{k})$ is expressed as

$$\Sigma\left(i\omega_n^f, \mathbf{k}\right) = \frac{1}{\beta}\sum_{\omega_m^b}\int \frac{d^3\mathbf{q}}{(2\pi)^3}\frac{\mathcal{G}\left(i\omega_m^b, \mathbf{q}\right)}{-i\omega_m^b + i\omega_n^f + \epsilon_{\mathbf{q}-\mathbf{k}} - \mu}. \tag{8}$$

The corresponding retarded Green's functions are defined as usual as $\delta_{ij}\delta_{\sigma\sigma'}G_R(t,\mathbf{r}) = -i\theta(t)\langle\{\psi_{i\sigma}(t,\mathbf{r}), \psi^\dagger_{j\sigma'}(0,0)\}\rangle$ and $\mathcal{G}_R(t,\vec{r}) = -i\theta(t)\langle[\varphi(t,\vec{r}), \bar{\varphi}(0,0)]\rangle$, where $\theta(t)$ is the heaviside step function. In momentum space, the forms of the retarded Green's functions can be obtained by the analytic continuation of Eqs. (5) and (7) as $\mathcal{G}_R(\omega,\mathbf{k}) = \mathcal{G}(i\omega_n^b \to \omega + i0^+, \mathbf{k})$ and $G_R(\omega,\mathbf{k}) = -G(i\omega_n^f \to \omega + i0^+, \mathbf{k})$. Then $G_R(\omega,\mathbf{k})$ is written as

$$G_R(\omega,\mathbf{k}) = \frac{-1}{-\omega - i0^+ + \epsilon_{\mathbf{k}} - \mu - \Sigma(\omega + i0^+, \mathbf{k})}. \tag{9}$$

Hence, in the dressed retarded Green's function, the pole is modified by the self-energy. Working to the first order in Σ, the pole can be approximately calculated as $\omega^* = \epsilon_{\mathbf{k}} - \mu - \mathrm{Re}\,\Sigma(\epsilon_{\mathbf{k}} - \mu + i0^+, \mathbf{k}) + i\Gamma(k)$, and the quantum scattering rate $\Gamma(k)$ is defined as $\Gamma(k) \equiv -\mathrm{Im}\,\Sigma(\epsilon_{\mathbf{k}} - \mu + i0^+, \mathbf{k})$.

To evaluate the OTOC, we need to define the symmetrized Wightman function as

$$\begin{aligned}\delta_{ij}\delta_{\sigma\sigma'}G_W(t,\mathbf{r}) &= \mathrm{Tr}\{\sqrt{\rho}\psi_{i\sigma}(t,\mathbf{r})\sqrt{\rho}\psi^\dagger_{i\sigma}(0,0)\},\\ \mathcal{G}_W(t,\mathbf{r}) &= \mathrm{Tr}\{\sqrt{\rho}\varphi(t,\mathbf{r})\sqrt{\rho}\bar{\varphi}(0,0)\}.\end{aligned} \tag{10}$$

In the momentum space, they can be written in terms of the spectral functions of fields $\psi_{i\sigma}$ and φ as

$$\begin{aligned}G_W(\omega,\mathbf{k}) &= \frac{A_F(\omega,\mathbf{k})}{2\cosh(\omega\beta/2)},\\ \mathcal{G}_W(\omega,\mathbf{k}) &= \frac{A_B(\omega,\mathbf{k})}{2\sinh(\omega\beta/2)}.\end{aligned} \tag{11}$$

The spectral functions can be calculated as the imaginary parts of the retarded Green's functions $A_F(\omega,\mathbf{k}) = -2\,\mathrm{Im}\,G_R(\omega,\mathbf{k})$ and $A_B(\omega,\mathbf{k}) = -2\,\mathrm{Im}\,\mathcal{G}_R(\omega,\mathbf{k})$.

III. THE LYAPUNOV EXPONENT

To calculate the Lyapunov exponent, it's convenient to evaluate the regulated squared anticommutator defined as [19,24]

$$\begin{aligned}\mathcal{C}_1(t) = \frac{\theta(t)}{N^2}\sum_{i,j}\int d^3\mathbf{r}\mathrm{Tr}[\sqrt{\rho}\{\psi_{i\uparrow}(t,\mathbf{r}), \psi^\dagger_{j\uparrow}(0,0)\}\\ \times\sqrt{\rho}\{\psi_{i\uparrow}(t,\mathbf{r}), \psi^\dagger_{j\uparrow}(0,0)\}^\dagger].\end{aligned} \tag{12}$$

The factor $1/N^2$ is to normalized the summation of indices i, j. Since the system is symmetric about exchanging spin indices, without losing any generality we investigate the regulated squared anticommutator of field $\psi_{i\uparrow}$ as above. For the calculation up to the order of $1/N$ the squared anticommutator $\mathcal{C}_1$ will couple to another squared anticommutator $\mathcal{C}_2$ as demonstrated in Fig. 2(c). The squared anticommutator $\mathcal{C}_2$ is written as the following:

$$\begin{aligned}\mathcal{C}_2(t) = \frac{\theta(t)}{N^2}\sum_{i,j}\int d^3\mathbf{r}\mathrm{Tr}[\sqrt{\rho}\{\psi^\dagger_{i\downarrow}(t,\mathbf{r}), \psi^\dagger_{j\uparrow}(0,0)\}\\ \times\sqrt{\rho}\{\psi^\dagger_{i\downarrow}(t,\mathbf{r}), \psi^\dagger_{j\uparrow}(0,0)\}^\dagger].\end{aligned} \tag{13}$$

At the moment of $t = 0$, the above anticommutators vanish because of $\mathbf{r} \neq 0$. However, in chaotic systems, the time evolution of the operators may involve increasing degrees of freedom. As a result, the fields become nonlocal at a later time. It is conjectured that the squared anticommutators will have an exponential growth $\mathcal{C}_i(t) \sim e^{\lambda_L t}$ at short time. Analogous to the approach in Ref. [18], to compute the λ_L to the leading order in $1/N$, we only keep the fastest-growing diagrams, which is a set of ladder diagrams as shown in Fig. 2(c). The "rails" of the ladder correspond to the retarded Green's functions. They are defined on the two real timefolds. The two rails are separated by an imaginary time difference $i\beta/2$ and they are connected by "rungs". The rungs correspond to the Wightman Green's functions.

The Fourier transformation of $\mathcal{C}_i(t)$ is denoted as $\mathcal{C}_i(\omega)$ with $\mathcal{C}_i(t) = \int d\omega e^{-i\omega t}\mathcal{C}_i(\omega)$. To sum up all the ladder series, it's convenient to define functions $f_i(\nu;\omega,\mathbf{k})$ as

$$\mathcal{C}_i(\nu) = \frac{1}{N}\int\frac{d\omega d^3\mathbf{k}}{(2\pi)^4}f_i(\nu;\omega,\mathbf{k}). \tag{14}$$

The lowest order of $f_1(\nu;\omega,\mathbf{k})$ is simply expressed as $G_R(\omega,\mathbf{k})G_R^*(\omega-\nu,\mathbf{k})$. Summation of all the ladder diagrams yields the Bethe-Salpeter equations,

$$\begin{aligned}f_1(\nu;\omega,\mathbf{k}) &= G_R(\omega,\mathbf{k})G_R^*(\omega-\nu,\mathbf{k})\Big(1 + \int\frac{d\omega' d^3\mathbf{k}'}{(2\pi)^4}\\ &\quad\times(\mathcal{K}_1(\nu;\omega,\mathbf{k};\omega',\mathbf{k}')f_2(\nu;\omega',\mathbf{k}')\\ &\quad+\mathcal{K}_2(\nu;\omega,\mathbf{k};\omega',\mathbf{k}')f_1(\nu;\omega',\mathbf{k}'))\Big),\\ f_2(\nu;\omega,\mathbf{k}) &= G_R(\omega,\mathbf{k})G_R^*(\omega-\nu,\mathbf{k})\\ &\quad\times\int\frac{d\omega' d^3\mathbf{k}'}{(2\pi)^4}\mathcal{K}_1(\nu;\omega,\mathbf{k};\omega',\mathbf{k}')f_1(\nu;\omega',\mathbf{k}'),\end{aligned} \tag{15}$$

where $\mathcal{K}_1$ and $\mathcal{K}_2$ are the integral kernels corresponding to the one-rung and two-rung diagrams in Fig. 2(c), respectively. They are written as

$$\begin{aligned}\mathcal{K}_1(\nu;\omega,\mathbf{k};\omega',\mathbf{k}') &= \mathcal{G}_W(\omega'+\omega,\mathbf{k}+\mathbf{k}'),\\ \mathcal{K}_2(\nu;\omega,\mathbf{k};\omega',\mathbf{k}')&\\ &= N\int\frac{d\omega'' d^3\mathbf{k}''}{(2\pi)^4}\mathcal{G}_R(\omega'',\mathbf{k}'')\mathcal{G}_R^*(\omega''-\nu,\mathbf{k}'')\\ &\quad\times G_W(\omega+\omega'',\mathbf{k}+\mathbf{k}'')G_W(\omega'+\omega'',\mathbf{k}'+\mathbf{k}'').\end{aligned} \tag{16}$$

For the following calculation, we will take several approximations. First, one expects the $f_1(\nu;\omega,\mathbf{k})$ to be exponentially growing, while the first term of f_1 in Eq. (15) will be decaying. Hence, this term can be safely dropped without affecting the evaluation of the growth rate. Second, the pair of fermionic Green's functions $G_R(\omega,\mathbf{k})G_R^*(\omega-\nu,\mathbf{k})$ in Eq. (15) can be

approximated as $\frac{2\pi i\delta(\omega-\epsilon_{\mathbf{k}}+\mu)}{\nu+2i\Gamma(k)}$. Third, because in the above approximation all pairs of the retarded Green's functions include an on-shell delta function, it's natural to postulate the on-shell form of $f_i(\nu;\omega,\mathbf{k})$ as $f_i(\nu;\omega,\mathbf{k})\approx f_i(\nu;\mathbf{k})\delta(\omega-\epsilon_{\mathbf{k}}+\mu)$ [18,19]. Please refer to Appendix A for the details of the approximation. With all above approximations, the Bethe-Saltpeter equations of Eq. (15) can be reduced to

$$\begin{aligned}&[-i\omega+2T\tilde{\Gamma}(\tilde{k})]f_1(\omega;\tilde{k})\\&=\frac{T}{N}\int\frac{d\tilde{k}'\tilde{k}'}{\tilde{k}}(\tilde{\mathcal{K}}_1(\tilde{k},\tilde{k}')f_2(\omega;\tilde{k}')+\tilde{\mathcal{K}}_2(\tilde{k},\tilde{k}')f_1(\omega;\tilde{k}')),\\&[-i\omega+2T\tilde{\Gamma}(\tilde{k})]f_2(\omega;\tilde{k})=\frac{T}{N}\int\frac{d\tilde{k}'\tilde{k}'}{\tilde{k}}\tilde{\mathcal{K}}_1(\tilde{k},\tilde{k}')f_1(\omega;\tilde{k}'),\end{aligned}\tag{17}$$

where the momenta have been rescaled to be dimensionless as $\tilde{k}=k/\sqrt{T}$ and $\tilde{k}'=k'/\sqrt{T}$. Correspondingly, we define a dimensionless quantum scattering rate $\tilde{\Gamma}=\Gamma/T$. Here we have assumed the function $f(\omega,\mathbf{k})$ is rotationally invariant and integrated over the angles. Then the function $f_i(\omega,\mathbf{k})$ is reduced to $f_i(\omega,k)$ in Eq. (17). The dimensionless functions $\tilde{\mathcal{K}}_1$ and $\tilde{\mathcal{K}}_2$ are written as

$$\begin{aligned}\tilde{\mathcal{K}}_1(\tilde{k},\tilde{k}')&=N\int_{|\tilde{k}'-\tilde{k}''|}^{\tilde{k}'+\tilde{k}''}\frac{\tilde{p}d\tilde{p}}{(2\pi)^2}\tilde{\mathcal{G}}_W(\tilde{\epsilon}_{k'}+\tilde{\epsilon}_{k''}-2\tilde{\mu},\tilde{p}),\\\tilde{\mathcal{K}}_2(\tilde{k},\tilde{k}')&=N^2\int\frac{d\tilde{k}''d\tilde{\omega}''}{128\pi^5}\frac{|\tilde{\mathcal{G}}_R(\tilde{\omega}'',\tilde{k}'')|^2\Theta(\tilde{k},\tilde{k}',\tilde{k}'')}{\cosh\left(\frac{\tilde{\epsilon}_k-\tilde{\mu}-\tilde{\omega}''}{2}\right)\cosh\left(\frac{\tilde{\epsilon}_{k'}-\tilde{\mu}-\tilde{\omega}''}{2}\right)},\end{aligned}\tag{18}$$

where $\tilde{k}''=k''/\sqrt{T}$, $\tilde{\omega}''=\omega''/T$, $\tilde{\epsilon}_k=\epsilon_k/T$, and $\tilde{\mu}=\mu/T$ and the bosonic retarded Green's functions and Wightman function are also rescaled to be dimensionless by $\tilde{\mathcal{G}}_R=\sqrt{T}\mathcal{G}_R$ and $\tilde{\mathcal{G}}_W=\sqrt{T}\mathcal{G}_W$. The Θ function is defined as $\Theta(k,k',k'')=\theta(2k'k''+\epsilon_{\mathbf{k}''}-\mu+k''^2)\theta(2k'k''-\epsilon_{\mathbf{k}''}+\mu-k''^2)\theta(2kk''+\epsilon_{\mathbf{k}''}-\mu+k''^2)\theta(2kk''-\epsilon_{\mathbf{k}''}+\mu-k''^2)$.

To more easily solve for the Lyapunov exponent the Bethe-Saltpeter equations of Eq. (17) can be written in a simple form,

$$-i\omega\mathcal{F}(\omega;\tilde{k})=\frac{T}{N}\int d\tilde{k}'\mathcal{S}(\tilde{k},\tilde{k}')\mathcal{F}(\omega;\tilde{k}'),\tag{19}$$

where $\mathcal{F}^T(\omega;\tilde{k})=(\tilde{k}f_1(\omega;\tilde{k}),\tilde{k}f_2(\omega;\tilde{k}))$ and the dimensionless integral kernel $\mathcal{S}(\tilde{k},\tilde{k}')$ is defined as the following:

$$\begin{aligned}&\mathcal{S}(\tilde{k},\tilde{k}')\\&=\begin{pmatrix}\tilde{\mathcal{K}}_2(\tilde{k},\tilde{k}')-2N\tilde{\Gamma}(\tilde{k}')\delta(\tilde{k}-\tilde{k}') & \tilde{\mathcal{K}}_1(\tilde{k},\tilde{k}')\\ \tilde{\mathcal{K}}_1(\tilde{k},\tilde{k}') & -2N\tilde{\Gamma}(\tilde{k}')\delta(\tilde{k}-\tilde{k}')\end{pmatrix}.\end{aligned}\tag{20}$$

We do not know how to solve Eq. (19) analytically. However, it can be solved numerically by discretizing the momenta $\tilde{k}$ and $\tilde{k}'$ in the integral kernel $\mathcal{S}(\tilde{k},\tilde{k}')$. Then, the integral becomes the summation over the discrete momentum and Eq. (19) can be written as

$$-i\omega\mathcal{F}(\omega;\tilde{k}_i)=\frac{T}{N}\sum_{\tilde{k}_j}\mathcal{S}(\tilde{k}_i,\tilde{k}_j)\mathcal{F}(\omega;\tilde{k}_j),\tag{21}$$

where $\tilde{k}_i$ is the discrete momentum with a small internals. Obviously, $-i\omega$ is given by the eigenvalues of the kernel $\mathcal{S}(\tilde{k}_i,\tilde{k}_j)$ multiplied by a factor T/N. By examining Eqs. (18) and (20), it's straightforward to see that $\mathcal{S}(\tilde{k}_i,\tilde{k}_j)$ is a Hermitian matrix. The eigenvalues are all real. Then the Lyapunov exponent corresponds to the largest eigenvalue. Please refer to Appendix B for the details of the numerical calculation of the Lyapunov exponent.

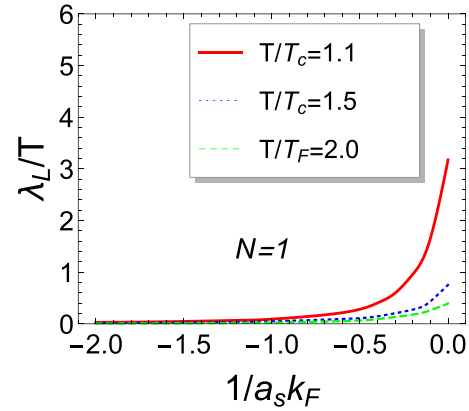

FIG. 3. λ_L/T as a function of $1/a_sk_F$. The red solid, the blue dotted, and the green dashed curves correspond to different temperatures $T/T_c=1.1$, 1.5, and 2.0, respectively, where $T_c=0.22T_F$.

IV. QUANTUM CHAOS AT THE UNITARY POINT

In this section, we study the case of unitary Fermi gases by setting $N=1$. This is not a fully controllable choice. However, since we only focus on the variations of the Lyapunov exponent with respect to the scattering length a_s and the temperature, it may generate qualitative correct interpretation as the large N cases and inspire useful insight. In Fig. 3, we plot λ_L/T as a function of $1/a_sk_F$ for fixed temperature $T/T_c=1.1$, 1.5, and 2.0, where $T_c=0.22T_F$ is the superfluid critical temperature at $1/a_sk_F=0$, which is calculated in the Nozières and Schmitt-Rink scheme [34,35]. One observes that the Lyapunov exponent monotonically increases as $1/a_sk_F$ goes from the BCS limit to the unitary regime. For lower temperature, the λ_L increases much faster than the higher temperature cases. At the unitary point $1/a_sk_F=0$, we plot λ_L/T as a function of temperature T/T_F in Fig. 4(a). As the temperature drops, the Lyapunov exponent monotonically increases and approaches the upper bound $2\pi T$. At the temperature $T/T_c=1.1$, the Lyapunov exponent can reach a value of $\lambda_L\approx 3.2T$. Here we would like to point out that we won't be able to explore the region further close to T_c for the $N=1$ case, where our numerical calculation becomes unstable. Please refer to Appendix B for details. The reason is that the propagator of the bosonic field φ in Eq. (5) is sensitive to the precision of the chemical potential μ as one approaches the critical temperature. For the case of larger N, the portion of preformed Cooper pairs becomes smaller and the calculation becomes less sensitive to the precision of the chemical potential. Hence, we would be able to calculate the Lyapunov exponent at T_c. In Figs. 4(b)–4(b), we plot $N\lambda_L/T$ as functions of temperature T/T_F for cases of $N=10$, 100, and ∞. For $N=10$, the calculation still cannot reach the critical temperature. However, for $N=100$ and

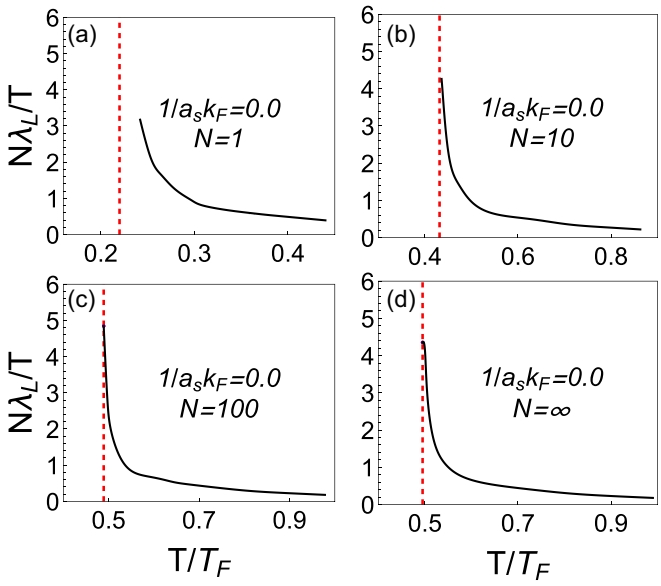

FIG. 4. (a)–(d) are the graphs of $N\lambda_L/T$ as a functions of temperature T/T_F at $1/a_sk_F = 0$ for $N = 1$, 10, 100, and ∞, respectively. The red dashed lines indicate the critical temperatures of the superfluid phase transitions for the four cases.

$N = \infty$, one observes that λ_L reaches a finite value at T_c and it obeys the bound of $2\pi/\beta$. Since there is no qualitative change from the $N = 1$ to $N = \infty$ cases, we believe λ_L/T will also reach a finite value at T_c for $N = 1$.

At the unitary point and temperature close to the critical point, the system possesses two features. First, the system is scaling invariant. It obeys the nonrelativistic conformal symmetry (the Schrödinger group). Investigations have been taken for the possible nonrelativistic version of ADS/CFT duality [27,28]. Second, it has been shown that around the critical temperature, the system demonstrates a behavior of non-Fermi liquid due to strong pairing fluctuations [30–33]. Some research has shown that certain systems lacking quasiparticle excitations demonstrate strong chaos [19,23,24,36,37]. Hence, it's not surprising that our system scrambles the fastest at the unitarity and the temperature close to T_c.

V. THE BEHAVIORS IN THE BCS LIMIT

At the BCS limit, the scattering length $a_s \to 0^-$. The retarded Green's function $\mathcal{G}_R$ of the field φ can be expanded in terms of small a_s as the following:

$$\mathcal{G}_R(\omega, \mathbf{k}) = \frac{1/N}{-\frac{m}{4\pi a_s} + \int \frac{d^3\mathbf{k}}{(2\pi)^3}\frac{1}{2\epsilon_{\mathbf{k}}} - \int \frac{d^3\mathbf{k}}{(2\pi)^3}\frac{1-n_F(\epsilon_{\mathbf{k}}-\mu)-n_F(\epsilon_{\mathbf{q}-\mathbf{k}}-\mu)}{-\omega-i0^+ +\epsilon_{\mathbf{k}}+\epsilon_{\mathbf{q}-\mathbf{k}}-2\mu}} \propto a_s/N. \tag{22}$$

Notice that the temperature must be far from the critical temperature. Otherwise, according to the Thouless criterion, one has $-\frac{m}{4\pi a_s} + \int \frac{d^3\mathbf{k}}{(2\pi)^3}\frac{1}{2\epsilon_{\mathbf{k}}} - \int \frac{d^3\mathbf{k}}{(2\pi)^3}\frac{1-n_F(\epsilon_{\mathbf{k}}-\mu)-n_F(\epsilon_{\mathbf{q}-\mathbf{k}}-\mu)}{-\omega+\epsilon_{\mathbf{k}}+\epsilon_{\mathbf{q}-\mathbf{k}}-2\mu} \to 0$ when T approaches T_c and $\mathcal{G}_R$ cannot be expanded for small a_s. Furthermore, since the Wightman function $\mathcal{G}_W$ and the quantum scattering rate $\Gamma(k)$ can be calculated by $\mathcal{G}_W(\omega, \mathbf{k}) = \frac{-\mathrm{Im}\,\mathcal{G}_R(\omega,\mathbf{k})}{\sinh(\omega\beta/2)}$ and $\Gamma(k) = \int \frac{d^3\mathbf{q}}{2(2\pi)^3}\mathcal{G}_W(\epsilon_{\mathbf{k}} + \epsilon_{\mathbf{q}-\mathbf{k}} - 2\mu, \mathbf{q})\frac{\cosh[(\epsilon_{\mathbf{k}}-\mu)/2T]}{\cosh[(\epsilon_{\mathbf{q}-\mathbf{k}}-\mu)/2T]}$, their behaviors for small a_s can be easily derived as $\mathcal{G}_R \propto za_s^2\sqrt{T}/N$ and $\Gamma(k) \propto za_s^2T^2/N$, where $z \equiv \exp(\mu/T)$ is the fugacity. Please refer to Appendix C for details. $\tilde{\mathcal{K}}_1(\tilde{k}, \tilde{k}')$ and $\tilde{\mathcal{K}}_2(\tilde{k}, \tilde{k}')$ in the integral kernel of Eq. (20) are functions of $\mathcal{G}_R$ and $\mathcal{G}_W$ as shown in Eq. (18). Then it's straightforward to obtain the behaviors as $\tilde{\mathcal{K}}_1(\tilde{k}, \tilde{k}') \propto za_s^2T$ and $\tilde{\mathcal{K}}_2(\tilde{k}, \tilde{k}') \propto za_s^2T$. The three terms in Eq. (20) all have the same asymptotic form of za_s^2T. Hence, as $a_s \to 0^-$, the Lyapunov exponent behaves as $\lambda_L \propto za_s^2T^2/N$, which is consistent with the results on the Fermi liquid theory with well-defined quasiparticles [29,38,39].

VI. CONCLUSIONS

We have computed the Lyapunov exponent for an N-flavor Fermion system using $1/N$ expansion. The variation of the Lyapunov exponent with respect to the scattering length a_s and temperature T has been investigated. When T is fixed, the Lyapunov exponent monotonically increases as the $1/a_sk_F$ increases from the BCS limit to the unitary regime. When the scattering length is fixed to $1/a_sk_F = 0$, the Lyapunov exponent increases while the temperature drops. Around the critical temperature, it can reach to the order of $\lambda_L \sim T$ for the $N = 1$ case. Basically, our results indicate that with strong pairing fluctuations the system exhibits strong chaos. Furthermore, the behavior of λ_L at the BCS limit was calculated as $\lambda_L \propto za_s^2T^2/N$, which is consistent with the Fermi liquid theory.

ACKNOWLEDGMENTS

We thank Shizhong Zhang, Yu Chen, and Pengfei Zhang for very helpful discussions. The work is supported by the National Science Foundation of China (Grant No. NSFC-11874002), Beijing Natural Science Foundation (Grant No. Z180007), and Hong Kong Research Grants Council, GRF No. 17304719, CRF No. C6026-16W, and No. C6005-17G.

APPENDIX A: APPROXIMATIONS FOR THE REDUCTION OF EQ. (17)

With the first approximation, the first term of f_1 in Eq. (15) is dropped. Then the Bethe-Salpeter equations in Eq. (15) is reduced to

$$\begin{aligned} f_1(\nu;\omega,\mathbf{k}) &= G_R(\omega,\mathbf{k})G_R^*(\omega-\nu,\mathbf{k})\int\frac{d\omega' d^3\mathbf{k}'}{(2\pi)^4} \\ &\quad\times(\mathcal{K}_1(\nu;\omega,\mathbf{k};\omega',\mathbf{k}')f_2(\nu;\omega',\mathbf{k}') \\ &\quad+\mathcal{K}_2(\nu;\omega,\mathbf{k};\omega',\mathbf{k}')f_1(\nu;\omega',\mathbf{k}')\,), \\ f_2(\nu;\omega,\mathbf{k}) &= G_R(\omega,\mathbf{k})G_R^*(\omega-\nu,\mathbf{k}) \\ &\quad\times\int\frac{d\omega' d^3\mathbf{k}'}{(2\pi)^4}\mathcal{K}_1(\nu;\omega,\mathbf{k};\omega',\mathbf{k}')f_1(\nu;\omega',\mathbf{k}'). \end{aligned} \tag{A1}$$

The second approximation is performed on the pair propagators $G_R(\omega, \mathbf{k})G_R^*(\omega - \nu, \mathbf{k})$. In the free fermion case, it's

expressed as

$$G_R(\omega,\mathbf{k})G_R^*(\omega-\nu,\mathbf{k}) = \frac{1}{\omega-\epsilon_{\mathbf{k}}+\mu+i0^+}\frac{1}{\omega-\nu-\epsilon_{\mathbf{k}}+\mu-i0^+}. \quad \text{(A2)}$$

The integration over ω can be evaluated by the method of residue. Then it's straightforward to yield

$$G_R(\omega,\mathbf{k})G_R^*(\omega-\nu,\mathbf{k}) = \frac{2\pi i\delta(\omega-\epsilon_{\mathbf{k}}+\mu)}{\nu+2i0^+}. \quad \text{(A3)}$$

The approximation is taken by replacing the 0^+ by the scattering rate $\Gamma(k)$ for the interacting case. Then,

$$G_R(\omega,\mathbf{k})G_R^*(\omega-\nu,\mathbf{k}) = \frac{2\pi i\delta(\omega-\epsilon_{\mathbf{k}}+\mu)}{\nu+2i\Gamma(k)}. \quad \text{(A4)}$$

As discussed in the main text, the third approximation is to postulate the on-shell form $f_i(\nu;\omega,\mathbf{k}) \approx f_i(\nu;\mathbf{k})\delta(\omega-\epsilon_{\mathbf{k}}+\mu)$. Then the Eq. (A1) can be written as

$$\begin{aligned}&[-i\nu+2\Gamma(k)]f_1(\nu;\mathbf{k})\\ &= \int\frac{d\omega' d^3\mathbf{k}'}{(2\pi)^4}2\pi\delta(\omega-\epsilon_{\mathbf{k}}+\mu)(\mathcal{K}_1(\nu;\omega,\mathbf{k};\omega',\mathbf{k}')f_2(\nu;\mathbf{k}')\\ &\quad +\mathcal{K}_2(\nu;\omega,\mathbf{k};\omega',\mathbf{k}')f_1(\nu;\mathbf{k}')), [-i\nu+2\Gamma(k)]f_2(\nu;\mathbf{k})\\ &= \int\frac{d\omega' d^3\mathbf{k}'}{(2\pi)^4}2\pi\delta(\omega-\epsilon_{\mathbf{k}}+\mu)\mathcal{K}_1(\nu;\omega,\mathbf{k};\omega',\mathbf{k}')f_1(\nu;\mathbf{k}').\end{aligned} \quad \text{(A5)}$$

Assuming $f_i(\nu;\mathbf{k}')$ is rotationally invariant and performing the integration by implementing the delta function $\delta(\omega-\epsilon_{\mathbf{k}}+\mu)$, one obtains the Eq. (17).

APPENDIX B: REMARKS ON NUMERICAL TECHNIQUE

To numerically solve for the Lyapunov exponent, we first discretize the momenta $\tilde{k}$ and $\tilde{k}'$ of the integral kernel $\mathcal{S}(\tilde{k},\tilde{k}')$ in Eq. (20) into N_{size} pieces. The cutoffs of momenta $\tilde{k}$ and $\tilde{k}'$ are set to $\Lambda = 15$. We have also checked the convergence of the results by performing the calculation for larger cutoffs. The kernel $\mathcal{S}(\tilde{k},\tilde{k}')$ is symmetric for exchanging $\tilde{k}$ and $\tilde{k}'$. Then it can be easily diagonalized to obtain the eigenvalues, which are denoted as λ_i here. The Lyapunov exponent is related to the largest eigenvalue as $\lambda_L N/T = \max(\lambda_i)$. Then the same calculation is performed for different N_{size} and the corresponding value of $\lambda_L N/T$ is obtained. As an example, we illustrate the case of $1/a_s k_F = 0$ and $T/T_c = 1.1$ in Fig. 5(a). The final value of $\lambda_L N/T$ is read by the extrapolation to $1/N_{\text{size}} = 0$. In Fig. 5(b), we present the extrapolation of the case $T/T_c = 1.04$, where one observes that squared residuals are large and hence the numerical calculation is unreliable.

APPENDIX C: BEHAVIORS AT BCS LIMIT

At the BCS limit, one has $a_s^{-1} \to -\infty$. Then the asymptotic behaviors of various propagators and the scattering rate $\Gamma(k)$ are demonstrated as the following. The full propagator of field φ is

$$\mathcal{G}_R(\omega,\mathbf{k}) = \frac{1/N}{1/g-\Pi(\omega,\mathbf{k})} \equiv \frac{1/N}{\text{Re}+i\text{Im}}, \quad \text{(C1)}$$

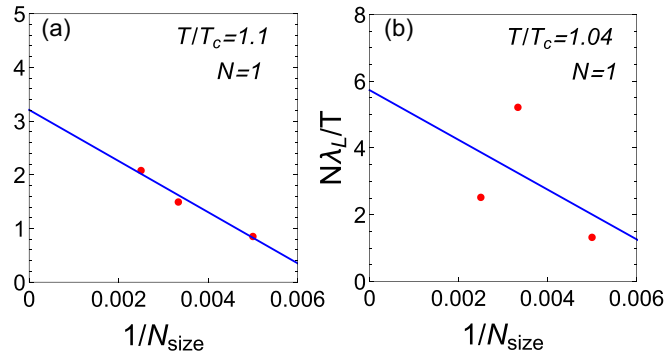

FIG. 5. The extrapolation of λ_L/T as a function of the discretized interval $1/N_{\text{size}}$. Graphs (a) and (b) are for the cases of $T/T_c = 1.1$ and 1.04, respectively, and $1/a_s k_F = 0$ in both graphs.

where

$$\begin{aligned}\text{Re} &= -\frac{m}{4\pi a_s}+\int\frac{d^3\mathbf{k}}{(2\pi)^3}\frac{1}{2\epsilon_{\mathbf{k}}}\\ &\quad -\int\frac{d^3\mathbf{k}}{(2\pi)^3}\frac{1-n_F(\epsilon_{\mathbf{k}}-\mu)-n_F(\epsilon_{\mathbf{q}-\mathbf{k}}-\mu)}{-\omega+\epsilon_{\mathbf{k}}+\epsilon_{\mathbf{q}-\mathbf{k}}-2\mu},\\ \text{Im} &= -\pi\int\frac{d^3\mathbf{k}}{(2\pi)^3}[1-n_F(\epsilon_{\mathbf{k}}-\mu)-n_F(\epsilon_{\mathbf{q}-\mathbf{k}}-\mu)]\\ &\quad\times\delta(-\omega+\epsilon_{\mathbf{k}}+\epsilon_{\mathbf{q}-\mathbf{k}}-2\mu).\end{aligned} \quad \text{(C2)}$$

After we rescale all the momenta and frequency by $\mathbf{k}\to k/\sqrt{T}$, $\mathbf{q}\to\mathbf{q}/\sqrt{T}$, and $\omega\to\omega/T$, it's straightforward to get the following asymptotic behaviors for large a_s^{-1}:

$$\begin{aligned}\text{Re} &\propto a_s^{-1},\\ \text{Im} &\propto \sqrt{T}.\end{aligned} \quad \text{(C3)}$$

Notice that the temperature here must be far from the superfluid critical temperature, otherwise $\text{Re}\to 0$. Then for large a_s^{-1} the propagator $\mathcal{G}_R(\omega,\mathbf{k})$ behaves as

$$\mathcal{G}_R(\omega,\mathbf{k}) \propto a_s/N. \quad \text{(C4)}$$

The imaginary part of $\mathcal{G}_R(\omega,\mathbf{k})$ is

$$\text{Im}\,\mathcal{G}_R(\omega,\mathbf{k}) = -\frac{1}{N}\frac{\text{Im}}{\text{Re}^2+\text{Im}^2} \propto a_s^2\sqrt{T}/N. \quad \text{(C5)}$$

The Wightman function of field φ behaves as

$$\begin{aligned}\mathcal{G}_W(\omega_k-2\mu,\mathbf{k}) &\equiv \frac{A_B(\omega_k-2\mu,\mathbf{k})}{2\sinh[(\omega_k-2\mu)\beta/2]}\\ &= \frac{-\text{Im}\,\mathcal{G}_R(\omega_k-2\mu,\mathbf{k})}{\sinh[(\omega_k-2\mu)\beta/2)]}\\ &\propto z a_s^2\sqrt{T}/N.\end{aligned} \quad \text{(C6)}$$

The self-energy of fermions is

$$\Sigma(i\omega_n^f,\mathbf{k}) = \frac{1}{\beta}\sum_{\omega_m^b}\int\frac{d^3\mathbf{q}}{(2\pi)^3}\frac{\mathcal{G}(i\omega_m^b,\mathbf{q})}{-i\omega_m^b+i\omega_n^f+\epsilon_{\mathbf{q}-\mathbf{k}}-\mu}, \quad \text{(C7)}$$

where the summation over ω_m^b is equivalent to a contour integration as the following:

$$\Sigma(i\omega_n^f, \mathbf{k}) = \int \frac{d^3\mathbf{q}}{(2\pi)^3}\Big(\int \frac{dz}{2\pi i}\frac{n_B(z)(\mathcal{G}_R(z,\mathbf{q}) - \mathcal{G}_A(z,\mathbf{q}))}{-z + i\omega_n^f + \epsilon_{\mathbf{q}-\mathbf{k}} - \mu} - \mathcal{G}\big(i\omega_n^f + \epsilon_{\mathbf{q}-\mathbf{k}} - \mu, \mathbf{q}\big)n_F(\epsilon_{\mathbf{q}-\mathbf{k}} - \mu)\Big), \quad \text{(C8)}$$

where $\mathcal{G}_A$ is the advanced Green's function for field φ. After we take a analytical continuation, the imaginary part of the self-energy can be calculated as

$$\begin{aligned}
&\mathrm{Im}\,\Sigma(\omega + i0^+, \mathbf{k}) \\
&= -\int \frac{d^3\mathbf{q}}{2(2\pi)^3}\Big(n_F(\epsilon_{\mathbf{q}-\mathbf{k}} - \mu)A_B(\omega + \epsilon_{\mathbf{q}-\mathbf{k}} - \mu) \\
&\quad + \int dz A_B(z)\delta(-z + \omega + \epsilon_{\mathbf{q}-\mathbf{k}} - \mu)n_B(z)\Big) \\
&= -\int \frac{d^3\mathbf{q}}{2(2\pi)^3}\mathcal{G}_W(\omega + \epsilon_{\mathbf{q}-\mathbf{k}} - \mu, \mathbf{q})\frac{\cosh\left(\frac{\omega}{2T}\right)}{\cosh\left(\frac{\epsilon_{\mathbf{q}-\mathbf{k}} - \mu}{2T}\right)}.
\end{aligned} \quad \text{(C9)}$$

The quantum scattering rate is defined as $\Gamma(k) = -\,\mathrm{Im}\,\Sigma(\epsilon_{\mathbf{k}} - \mu + i0^+, \mathbf{k})$. Then it can be written as

$$\Gamma(k) = \int \frac{d^3\mathbf{q}}{2(2\pi)^3}\mathcal{G}_W(\epsilon_{\mathbf{k}} + \epsilon_{\mathbf{q}-\mathbf{k}} - 2\mu, \mathbf{q})\frac{\cosh\left(\frac{\epsilon_{\mathbf{k}} - \mu}{2T}\right)}{\cosh\left(\frac{\epsilon_{\mathbf{q}-\mathbf{k}} - \mu}{2T}\right)}. \quad \text{(C10)}$$

As we have derived in Eq. (C6), the asymptotic behavior of the Wightman function is $\mathcal{G}_W(\epsilon_{\mathbf{k}} + \epsilon_{\mathbf{q}-\mathbf{k}} - 2\mu, \mathbf{q}) \propto z a_s^2\sqrt{T}/N$, then the asymptotic behavior of the quantum scattering rate for large a_s^{-1} is as the following:

$$\Gamma(k) \propto z a_s^2 T^2/N. \quad \text{(C11)}$$

With all above asymptotic forms of $\mathcal{G}_R(\omega, \mathbf{k})$, $\mathcal{G}_W(\omega, \mathbf{k})$, and $\Gamma(k)$, straightforward calculation yields

$$\begin{aligned}
\tilde{\mathcal{K}}_1(\tilde{k}, \tilde{k}') &\propto z a_s^2 T, \\
\tilde{\mathcal{K}}_2(\tilde{k}, \tilde{k}') &\propto z a_s^2 T,
\end{aligned} \quad \text{(C12)}$$

and hence

$$\mathcal{S}(\tilde{k}, \tilde{k}') \propto z a_s^2 T. \quad \text{(C13)}$$

Then the asymptotic behavior of Lyapunov exponent λ_L for large a_s^{-1} is

$$\lambda_L \propto T\left(z a_s^2 T\right)/N = z a_s^2 T^2/N. \quad \text{(C14)}$$

[1] Y. Sekino and L. Susskind, J. High Energy Phys. 10 (2008) 065.
[2] J. Maldacena, Adv. Theor. Math. Phys. **2**231 (1998); Int. J. Theor. Phys. **38**, 1113 (1999).
[3] S. S. Gubser, I. R. Klebanov, and A. M. Polyakov, Phys. Lett. B **428**, 105 (1998).
[4] E. Witten, Adv. Theor. Math. Phys. **2**, 253 (1998).
[5] S. H. Shenker and D. Stanford, J. High Energy Phys. 03 (2014) 067.
[6] D. A. Roberts, D. Stanford, and L. Susskind, J. High Energy Phys. 03 (2015) 051.
[7] S. H. Shenker and D. Stanford, J. High Energy Phys. 05 (2015) 132.
[8] A. Kitaev, Hidden correlations in the hawking radiation and thermal noise, talk given at Fundamental Physics Prize Symposium, in Proceedings of the Stanford SITP seminars, 2014, http://online.kitp.ucsb.edu/online/joint98/kitaev/.
[9] M. Rigol, V. Dunjko, and M. Olshanii, Nature (London) **452**, 854 (2008).
[10] T. Langen, R. Geiger, M. Kuhnert, B. Rauer, and J. Schmiedmayer, Nat. Phys. **9**, 640 (2013).
[11] A. M. Kaufman, M. E. Tai, A. Lukin, M. Rispoli, R. Schittko, P. M. Preiss, and M. Greiner, Science **353**, 794 (2016).
[12] A. I. Larkin and Yu. N. Ovchinnikov, J. Exp. Theor. Phys. **28**, 1200 (1969).
[13] J. Maldacena, S. H. Shenker, and D. Stanford, J. High Energy Phys. 08 (2016) 106.
[14] G. Zhu, M. Hafezi, and T. Grover, Phys. Rev. A **94**, 062329 (2016).
[15] N. Y. Yao, F. Grusdt, B. Swingle, M. D. Lukin, D. M. Stamper-Kurn, J. E. Moore, and E. Demler, arXiv:1607.01801.
[16] M. Gättner, J. G. Bohnet, A. Safavi-Naini, M. L. Wall, J. J. Bollinger, and A. M. Rey, Nat. Phys. **13**, 781 (2017).
[17] J. Li, R. Fan, H. Wang, B. Ye, B. Zeng, H. Zhai, X. Peng, and J. Du, Phys. Rev. X **7**, 031011 (2017).
[18] D. Stanford, J. High Energy Phys. 10 (2016) 009.
[19] D. Chowdhury and B. Swingle, Phys. Rev. D **96**, 065005 (2017).
[20] S. Sachdev and J. Ye, Phys. Rev. Lett. **70**, 3339 (1993).
[21] A. Kitaev, A simple model of quantum holography. KITP http://online.kitp.ucsb.edu/online/entangled15/kitaev/ (2015).
[22] J. Maldacena and D. Stanford, Phys. Rev. D **94**, 106002 (2016).
[23] Aavishkar A. Patel and S. Sachdev, Proc. Natl. Acad. Sci. USA **114**, 1844 (2017).
[24] S. Jian and H. Yao, arXiv:1805.12299.
[25] G. Bentsen, T. Hashizume, A. S. Buyskikh, E. J. Davis, A. J. Daley, S. S. Gubser, and M. Schleier-Smith, Phys. Rev. Lett. **123**, 130601 (2019).
[26] C. B. Da and L.-M. Duan, Phys. Rev. A **99**, 052322 (2019).
[27] K. Balasubramanian and J. McGreevy, Phys. Rev. Lett. **101**, 061601 (2008).
[28] D. T. Son, Phys. Rev. D **78**, 046003 (2008).
[29] P. Zhang, J. Phys. B: At., Mol. Opt. Phys. **52**, 135301 (2019).
[30] S. Krinner, M. Lebrat, D. Husmann, C. Grenier, J.-P. Brantut, and T. Esslinger, Proc. Natl. Acad. Sci. USA **113**, 8144 (2016).
[31] B. Liu, H. Zhai, and S. Zhang, Phys. Rev. A **95**, 013623 (2017).
[32] D. Husmann, M. Lebrat, S. Häusler, J.-P. Brantut, L. Corman, and T. Esslinger, Proc. Natl. Acad. Sci. USA **115**, 8563 (2018).
[33] X. Han, B. Liu, and J. Hu, Phys. Rev. A **100**, 043604 (2019).

[34] P. Nozières and S. Schmitt-Rink, J. Low Temp. Phys. **59**, 195 (1985).
[35] Y. Ohashi and A. Griffin, Phys. Rev. Lett. **89**, 130402 (2002).
[36] B. Swingle and T. Senthil, Phys. Rev. B **87**, 045123 (2013).
[37] S. A. Hartnoll, A. Lucas, and S. Sachdev, *Holographic Quantum Matter* (The MIT Press, 2018).
[38] Igor L. Aleiner, L. Faoro, and Lev B. Ioffe, Ann. Phys. **375**, 378 (2016).
[39] S. Banerjee and E. Altman, Phys. Rev. B **95**, 134302 (2017).